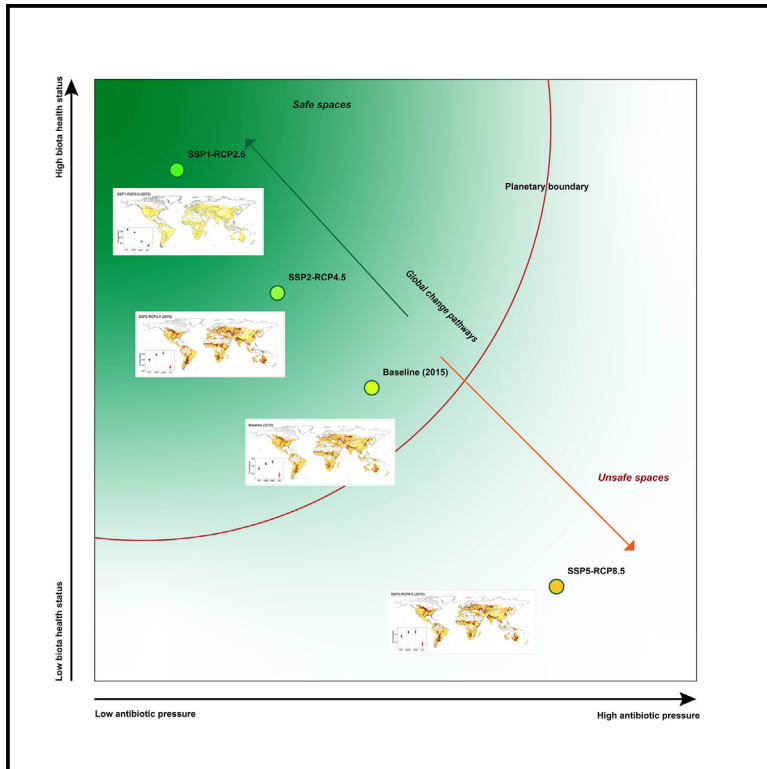


# Global prediction of agricultural soil antibiotic susceptibility and safe boundary for biota

## Graphical abstract



## Authors

Fangkai Zhao, Lei Yang, Yuanyuan Huang, ..., Long Sun, Min Li, Liding Chen

## Correspondence

leiyang@rcees.ac.cn (L.Y.),  
huangyy@igsnr.ac.cn (Y.H.),  
liding@ynu.edu.cn (L.C.)

## In brief

Microbiology; Agricultural science; Soil chemistry; Soil biology

## Highlights

- Agricultural soil antibiotic pollution poses planetary boundary threats to biota
- Global changes affect the geographical hotspots of antibiotic threats
- SSP5-RCP8.5 scenario pushes antibiotic pressures beyond the planetary boundaries



## Article

# Global prediction of agricultural soil antibiotic susceptibility and safe boundary for biota

Fangkai Zhao,<sup>1,2,3</sup> Lei Yang,<sup>2,5,\*</sup> Yuanyuan Huang,<sup>4,\*</sup> Haw Yen,<sup>6</sup> Yong Huang,<sup>7</sup> Qingyu Feng,<sup>2,5</sup> Long Sun,<sup>2,5</sup> Min Li,<sup>2,5</sup> and Liding Chen<sup>1,2,3,5,8,9,\*</sup>

<sup>1</sup>School of Ecology and Environmental Sciences, Yunnan University, Kunming, China

<sup>2</sup>State Key Laboratory for Ecological Security of Regions and Cities, Research Center for Eco-Environmental Sciences, Chinese Academy of Sciences, Beijing, China

<sup>3</sup>Ministry of Education Key Laboratory for Transboundary Ecoscience of Southwest China, Yunnan University, Kunming, China

<sup>4</sup>Institute of Geographic Sciences and Natural Resources Research, Chinese Academy of Sciences, Beijing, China

<sup>5</sup>University of Chinese Academy of Sciences, Beijing, China

<sup>6</sup>School of Forestry and Wildlife Sciences, Auburn University, Auburn, AL, USA

<sup>7</sup>Institute of International Rivers and Eco-security, Yunnan University, Kunming, China

<sup>8</sup>Southwest United Graduate School, Kunming, China

<sup>9</sup>Lead contact

\*Correspondence: [leiyang@rcees.ac.cn](mailto:leiyang@rcees.ac.cn) (L.Y.), [huangyy@igsrr.ac.cn](mailto:huangyy@igsrr.ac.cn) (Y.H.), [liding@ynu.edu.cn](mailto:liding@ynu.edu.cn) (L.C.)

<https://doi.org/10.1016/j.isci.2025.112066>

## SUMMARY

Pervasive anthropogenic activities release substantial quantities of antibiotics into soils, damaging soil organisms, introducing antibiotic resistance, and thus jeopardizing the safe boundaries for biodiversity. Here, by applying advanced geospatial modeling and establishing the planetary boundary (PB), we estimated that, at the baseline year (2015), global agricultural soil antibiotic concentration is  $122.0 \mu\text{g kg}^{-1}$ , within the PB of  $153.7 \mu\text{g kg}^{-1}$  beyond which the health of soil biota (including bacteria, fungi, invertebrates, and antibiotic-resistance genes) decreases dramatically. In  $\sim 2070$ , soil antibiotic concentrations increase while the boundaries decrease from SSP1-RCP2.6, SSP2-RCP4.5 to SSP5-RCP8.5. Under SSP5-RCP8.5, global soil organisms face the adverse antibiotic pollution ( $148.9 \mu\text{g kg}^{-1}$ ) that has transgressed the boundary ( $136.1 \mu\text{g kg}^{-1}$ ). Our study reveals the geopolitical inequality arising from antibiotic susceptibility and highlights the urgent need of the sustainable development to avoid catastrophic consequences on global soil organisms.

## INTRODUCTION

The widespread application of antibiotics during production, usage, and disposal practices (e.g., via wastewater irrigation, manure application, and waste landfilling)<sup>1–3</sup> has severely contaminated agricultural soils, triggering multiple interconnected ecological issues, such as disruptions in soil microbial communities, emergent antibiotic-resistant strains, reduced soil fertility and crop production, bioaccumulation within the food chain, and disturbances in ecosystem functioning and health.<sup>4–7</sup> Unfortunately, driven by the growing need for disease prevention, treatment, and livestock productivity, global antibiotic consumption and emissions are projected to increase further in the future.<sup>8,9</sup> Agricultural soil antibiotic pollution and susceptibility have been emerging as novel contributors to the transgression of critical safe boundaries, which refer to the thresholds of antibiotic contamination that must not be exceeded to avoid destabilizing soil biodiversity and the broader Earth system.<sup>10–12</sup> This underscores the urgency for focused attention and action in addressing this challenge.

Antibiotics significantly impact soil biota health by narrowing the safe boundaries for their survival.<sup>11</sup> These impacts can be categorized into three dimensions.<sup>4,13</sup> First, antibiotics inhibit the growth

of microorganisms and invertebrates, leading to species loss when exposure exceeds tolerance levels, thereby reducing soil biodiversity.<sup>14–16</sup> Second, antibiotics homogenize community structures by reducing dissimilarity as they suppress antibiotic-sensitive species while promoting resistant ones<sup>17</sup> making community assembly processes more uniform.<sup>18–20</sup> Third, antibiotic pollution increases resistance, enriching resistance genes that enable organisms to survive under antibiotic stress.<sup>21,22</sup> The wide presence of antibiotic resistance accelerates gene transfer, disrupts soil microbial diversity, and impairs ecosystem functions,<sup>11</sup> raising concerns about surpassing safety thresholds and jeopardizing soil biota and planetary health.<sup>23</sup> Despite multiple local-scale studies on antibiotic presence,<sup>24,25</sup> large scale data and insights into their impact on soil organisms remain insufficient. To comprehensively and quantitatively understand this issue, there is an urgent need for precise information on the spatial distribution and future changes of antibiotics and the related impacts, employing advanced assessment methods that consider not only antibiotic resistance but also biodiversity and community structure. Global information is crucial to evaluate the planetary-scale disruption caused by soil antibiotic pollution, pinpoint damage hotspots, comprehend the influence of future global changes on these relationships, and shape effective remediation policies. It plays a vital



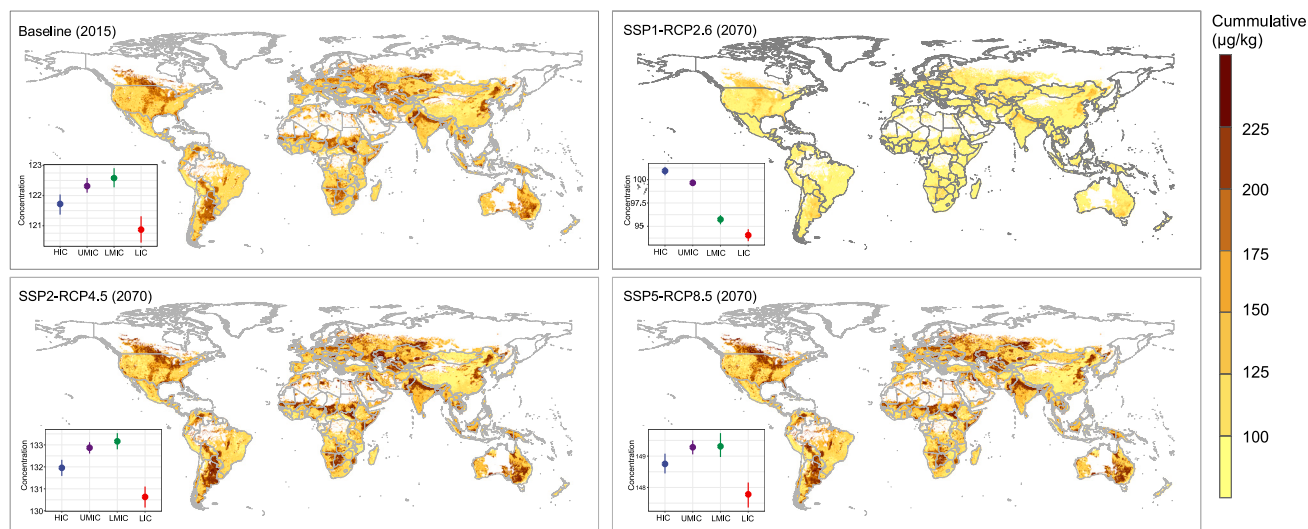


**Figure 1. Global maps of cumulative antibiotic concentrations in soil**

The cumulative concentration is the sum of target antibiotic concentrations per grid on the basis of the concentration addition principle.<sup>36</sup> The diagrams on the lower left of maps represent the average concentration of antibiotics in soil from different regions, and the points and error bars denote the average values and 95% confidence intervals. Country income levels are based on the World Bank. HIC, high-income countries; UMIC, upper-middle income countries; LMIC, lower-middle income countries; LIC, low-income countries. SSP1-RCP2.6, global sustainable future scenario; SSP2-RCP4.5, intermediate scenario; and SSP5-RCP8.5, high fossil fuel emission and business as usual scenario. The extent of agricultural land is from the ref.<sup>37</sup>

role in guiding societies toward development paths that proactively tackle the diverse challenges posed by antibiotic pollution.

Here, by compiling a global database with 1,351 soil samples across 659 unique locations covering a wide range of environmental conditions (from tropical to sub-frigid regions) and anthropogenic influences (from low-to high-income countries) across the Earth, we established machine learning models (see [STAR Methods](#), validation  $R^2$ : 0.47–0.59) linking the concentration of soil antibiotics (COSA in short, measured by the cumulative concentration of frequently detected antibiotics) with anthropogenic, climatic, soil, and topographic factors (see [STAR Methods](#)). In addition to quantifying the present-day (2015, baseline) COSA levels, we projected the future status of soil antibiotics, their impacts on soil organisms (including identify the hotspots) and assessed the threshold of COSA beyond which soil biota health decreases dramatically according to three future development scenarios,<sup>26,27</sup> combining the Shared Socioeconomic Pathways (SSPs) and Representative Concentration Pathways (RCPs), from SSP1-RCP2.6 (global sustainable scenario), SSP2-RCP4.5 (intermediate pathway) to SSP5-RCP8.5 (resource-intensive and fossil fuel development).<sup>28</sup> Considering the multidimensionality of responses of soil biota, we applied the standardized metric, B-DAR, which integrates Biodiversity (alpha diversity) and community Dissimilarity (bacteria, fungi, and invertebrates) together with Antibiotic Resistance to indicate the health status of soil biota (see [STAR Methods](#)).

## RESULTS AND DISCUSSION

### Global agricultural soil antibiotic pollution

We estimated the global COSA at present was  $122.0 \mu\text{g kg}^{-1}$  (95% confidence interval (CI):  $116.4\text{--}132.4 \mu\text{g kg}^{-1}$ ), exceeding

the current regional safe limit of  $100 \mu\text{g kg}^{-1}$  set by EU.<sup>29</sup> Despite the reliable performance of our four models, the projections show relatively high levels of uncertainty in the Northern Hemisphere (uncertainty <20%, [Figure S1](#)). High COSA exists in agricultural soils particularly with high coverages of crops (e.g., Southern of South America, Central Africa, India, East China, Northern United States, [Figure 1](#); [Figure S2](#)). This is often associated with intensive farming practices and crops such as rice and maize, which are frequently linked to high antibiotic use due to irrigation with wastewater, manure application, and other agricultural inputs.<sup>30</sup> Overall, soils in lower-middle income countries accumulate highest COSA, which is likely due to the increased antibiotic consumption and environmental emissions.<sup>8</sup> Lower-middle income countries generally have a high burden of infectious diseases (both humans and livestock animals) and a significant unmet need for antibiotics, which are paralleled by a life expectancy burden.<sup>8,31,32</sup> Even though high-income countries consume more antibiotics, the less regulated waste and wastewater treatment plants in lower-middle income countries lead to more severe soil antibiotic pollution.<sup>8,33</sup> Farmers in lower-middle income countries have typically deposited antibiotic-contaminated manure or wastewater onto agricultural land to improve soil productivity over the past three decades. For example, Asian land received 24.4–37.7% of global manure application, and this practice is growing at a rate of 0.47 Tg of nitrogen per decade.<sup>34</sup> This supports our finding that soil antibiotic pollution is more serious in Asia and Africa (particularly South Asia and North Africa, [Figure S2](#)). Our study, in line with earlier studies,<sup>1,29,35</sup> emphasizes that intensively managed agricultural soil generally has high antibiotic concentration.

Under the sustainable development scenario (SSP1-RCP2.6), there is an overall decrease in future (2070) soil antibiotic

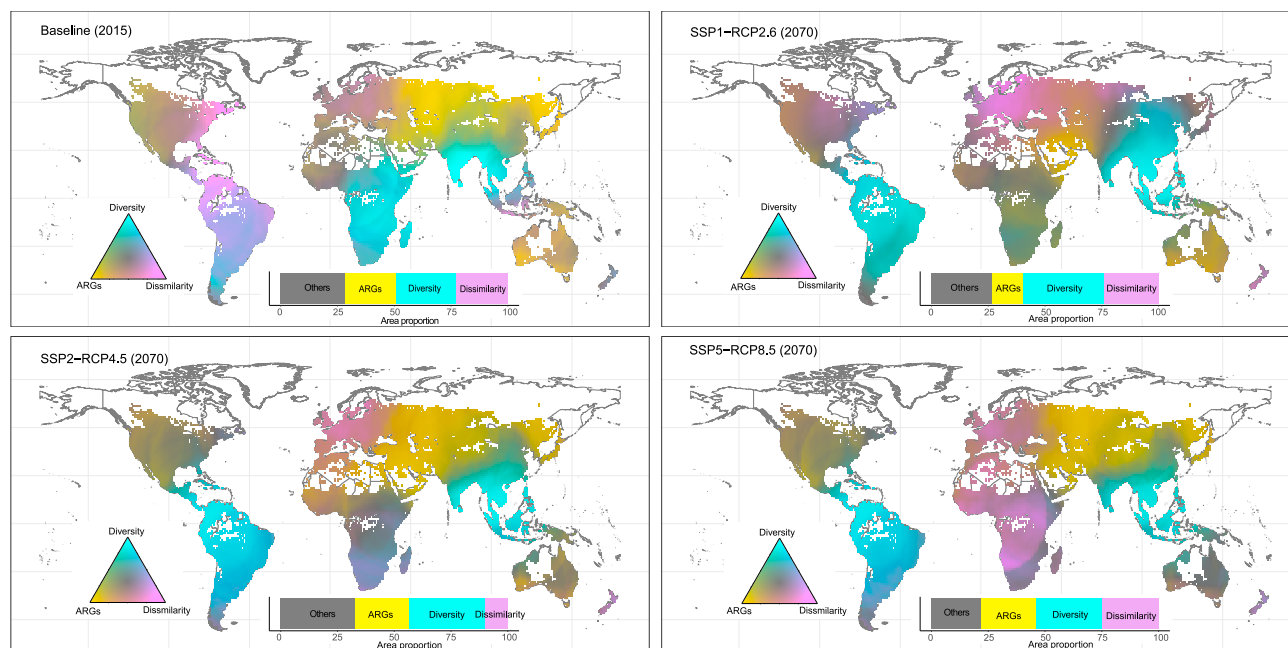


**Figure 2. Current and future three-dimensional hotspots of soil biota health linked to antibiotic pollution**

Diversity and dissimilarity indicate Getis-Ord z-scores of alpha diversity and community dissimilarity (Jaccard distance) of the soil biota, respectively, and antibiotic resistance genes (ARGs) is a Z score of antibiotic resistance gene richness. The Z score values for diversity and dissimilarity are reversed, given the widely negative effects of antibiotics (i.e., biodiversity loss and dissimilarity reductions). The color mixes represent high-probability hotspots of areas with maximal relationship strength between antibiotic concentration (COSA) and a given dimension and areas that allow for disturbance of the multi-dimensions of soil biota health under the same scenario. For example, the cyan color indicates that the probability that locations are hotspots of decreased alpha diversity is higher than that of decreased community dissimilarity and increased antibiotic resistance. Cumulative bar charts indicate hotspot area proportions (%) that maximize a given dimension. The gray color is a mix of all three dimensions, none of which dimension dominate the other.

concentration (mean:  $98.5 \mu\text{g kg}^{-1}$ , 95% CI:  $93.7\text{--}104.3 \mu\text{g kg}^{-1}$ ) likely due to the contraction of agricultural land area and a slow-down in population growth. Notably, soil antibiotic concentration is positively associated with economic development (Figure 1). This is in agreement with global patterns of antibiotic consumption, with wealthier countries having more access to goods (including antibiotics).<sup>8,38</sup> As the demand for antibiotics decreases due to fewer treatments required for infectious diseases like those related to enteropathogens, owing to sustainable urbanization and population growth,<sup>39</sup> low-income countries benefit most from SSP1-RCP2.6 with COSA decreasing by  $-33.1\%$ . Africa has the greatest decreases in COSA, ranging from  $-30.3\%$  to  $-35.6\%$  (Figure S2), partially caused by an increase in precipitation, which promoted the loss of antibiotics from soils by increasing surface runoff and soil erosion.<sup>27</sup>

By contrast, global COSA under the SSP2-RCP4.5 and SSP5-RCP8.5 increase to  $132.4 \mu\text{g kg}^{-1}$  (95% CI:  $125.3\text{--}142.6 \mu\text{g kg}^{-1}$ ) and  $148.9 \mu\text{g kg}^{-1}$  (95% CI:  $142.7\text{--}160.0 \mu\text{g kg}^{-1}$ ) respectively (Figure 1). Our analysis revealed the relatively high COSA of lower-middle income countries in these two scenarios, and the highest average COSA occur in South Asia and North Africa (Figure S2). However, upper-middle income countries experienced a more substantial increase in COSA (22% increase compared to the present-day baseline). Major increase was found in South America and Eastern Europe, where COSA increased by 22.7% (from  $134.9$  to  $165.5 \mu\text{g kg}^{-1}$ ) and 21.5% (from  $142.9$  to

$173.5 \mu\text{g kg}^{-1}$ ) under SSP5-RCP8.5 respectively. The increase in COSA is consistent with the increasing risk of exposure to bacterial diseases projected under these two future scenarios. For example, hotspots of *Vibrio* spp. in Eastern Europe<sup>40</sup> and of vector-borne pathogens in South America<sup>31</sup> are projected to occur, and these infections require large amounts of antibiotics for treatment and thus promote antibiotic emissions into the agricultural soil environment. Otherwise, the geographical similarity between soil antibiotic concentration and the mineral-associated soil organic carbon content in South America is suggested by our findings and a previous study,<sup>41</sup> possibly because of the adsorption of antibiotics by soil minerals.<sup>42</sup>

### Susceptibility of soil organisms to antibiotic pollution on a changing planet

Some soil ecosystems are susceptible to increased exposure to antibiotics and are characterized by their decreasing alpha diversity,<sup>16</sup> while others experienced alterations in their community structures or the spread of antibiotic resistance.<sup>43,44</sup> We employed geographically weighted regressions to estimate the impact strengths (regression slope) between soil antibiotic concentration (COSA) and different dimensions of biota status, and a Getis-Ord  $G_i^*$  spatial clustering algorithm to identify global hotspots<sup>45</sup> (see STAR Methods).

The dominance of the responses varies across regions (Figure 2). At the present-day, soil antibiotic pollution tends to



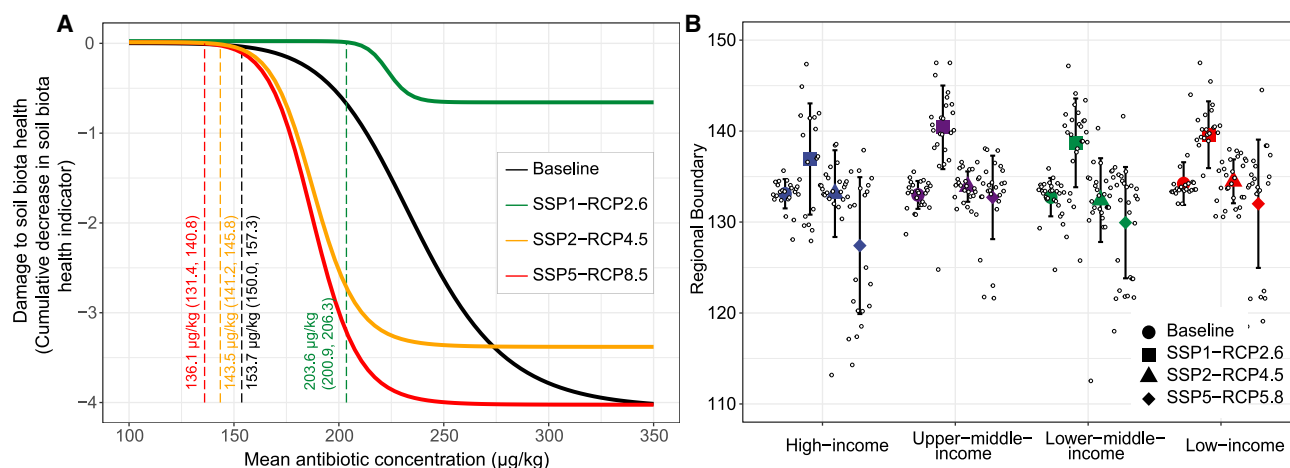


**Figure 3. Boundaries for soil antibiotic pollution**

(A) Curves of cumulative decrease in biota health (sum of impact strengths) against the soil antibiotic concentration from the top 0%–100% pixels. The boundary values are estimated by significant changes in linear relationship slopes. The mean estimates and 95% confidence intervals (values in brackets) for global boundaries are provided.

(B) Regional boundaries for different income levels. The colored points and error bars are the mean boundaries and 95% confidence intervals, respectively, and hollow points show the distribution of data.

negatively impact biodiversity in 26.8% of the global agricultural land, especially in South Asia and South Africa. Soil community dissimilarity is significantly altered in 22.6% of the global land including South America, western North America, and Eastern Europe. Soil bacterial diversity exhibits a higher proportion of hotspot areas than fungi and invertebrate diversities (Figure S3), which supports previous findings of high bacterial sensitivity to antibiotic exposure.<sup>16</sup> Our findings further suggest that bacterial and fungi communities respond to soil antibiotic pollution synergistically, i.e., there are large overlaps in their hotspots across space and time (Figure S4). Maximum probability of hotspot of antibiotic-induced resistance exists in contrasting regions, clustering in North and Central Asia, eastern North America, and Oceania (22.3%). In regions such as Oceania, there are higher probabilities of becoming global hubs for the spread of antibiotic resistance, as opposed to experiencing biodiversity loss or community homogenization, despite the clustering of hotspots with high antibiotic resistance impact did not reach statistical significance ( $p > 0.05$ , Figure 2; Figure S5). Although hotspots of antibiotic-induced changes in soil biodiversity, community dissimilarity, and antibiotic resistance have regional disparities, a wide range of locations display more than one of these dimensions (28.4% presently, Figure 2).

Furthermore, the hotspots of antibiotic impact on soil biota shift with global changes in the future (Figure 2), because of the changing antibiotic pressure and adaption of soil organisms.<sup>3,46</sup> We projected that, across all scenarios, biodiversity loss will spread to East and South Asia and South America, and high-probability area of biodiversity loss (with a coverage of 28.8–35.5% in the three future scenarios) will increase from 2015 to 2070, highlighting the increasing burden on soil biodiversity. In Africa, soil antibiotic pollution concurrently impacts biodiversity, community dissimilarity, and antibiotic resistance under SSP1-RCP2.6 and SSP2-RCP4.5 scenarios, while

SSP5-RCP8.5 mainly resulted in the highest hotspot probabilities of decreasing community dissimilarity. Community dissimilarity also decreases substantially in Europe across all scenarios. The multi-scenario comparison suggests that high-probability hotspots of antibiotic resistance are limited to 14.0% of evaluated land areas under SSP1-RCP2.6 (mainly in Central Asia and Oceania) and will increase to 24.1% under SSP2-RCP4.5 and 24.6% under SSP5-RCP8.5, mostly clustering in Central Asia. Antibiotic pressures will be imposed on more than one of the dimensions of soil biota health across 32.6% of the global land under SSP2-RCP4.5. SSP5-RCP8.5 will generate more locations (mainly in Africa) with antibiotic pressure on one dimension, and less locations (21.8%) with pressure on all dimensions in comparisons with present-day and other two scenarios.

Altogether, the magnitudes of damage on soil biota health show strong regional variations (Figure S6) based on relationship strength between COSA and B-DAR. Currently, soil biota in South America is most susceptible to soil antibiotic pollution, with an average significant ( $|t| > 1.96$ ) impact slope of  $-0.016$  (per  $\mu\text{g kg}^{-1}$  of antibiotics). SSP1-RCP2.6 will result in generally smaller and weakly negative relationships between antibiotic concentration and biota health around 2070. South America, Mesoamerica, and South Africa are mostly classified as hotspot locations (ranking top 5) with high burdens of soil antibiotic impacts on soil biota under both SSP2-RCP4.5 and SSP5-RCP8.5 (Figure S6). These regions also are global hotspots for soil biodiversity and ecosystem services<sup>26</sup> and are where more efforts should be adopted to reduce antibiotic susceptibility.

### Safe boundaries of agricultural soil antibiotic pollution

Respecting current antibiotic pollution boundaries to avoid threats to soil biota health requires a global limit of COSA of  $153.7 \mu\text{g kg}^{-1}$  (95% CI:  $150.0$ – $157.3 \mu\text{g kg}^{-1}$ , Figure 3A). When only one of the three dimensions of soil biota is considered,

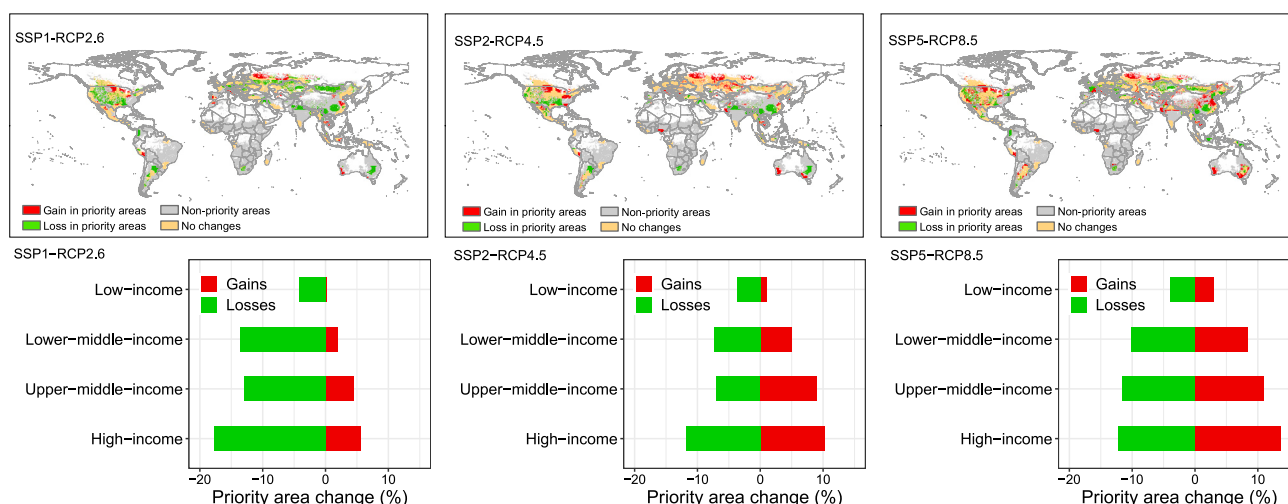


**Figure 4. Projected changes in the priority areas threatened by soil antibiotic pollution**

We defined priority areas as locations with two criteria: (1) soil antibiotic concentrations exceeding the boundary values and (2) significant impact strengths, i.e., the absolute *t* statistics exceed 1.96, as generated from geographically weighted regressions.

the current antibiotic pollution boundaries increase to  $163.6\text{--}166.3\ \mu\text{g kg}^{-1}$  (Figure S7). Multi-dimensional comprehensive criterion requires more strict control of antibiotic susceptibility. With altered antibiotic pollution burden and evolution of organisms, some soil biota surviving under the current antibiotic pollution boundaries lose their tolerances in the future, and the current safe threshold may fail to protect soil biota health, which is similar to the example of changing carbonate boundaries for coral reefs.<sup>47</sup> In this case, lower antibiotic pollution boundaries is needed to sustain soil biota. In line with previous findings,<sup>26</sup> we found that SSP5-RCP8.5 was the most stringent scenario for soil biota health, requiring the strongest reductions in global soil antibiotic pollution (lower than  $136.1\ \mu\text{g kg}^{-1}$ ; 95% CI:  $131.4\text{--}140.8\ \mu\text{g kg}^{-1}$ ). SSP1-RCP2.6 brings a larger safe boundary ( $203.6\ \mu\text{g kg}^{-1}$ , 95% CI:  $200.9\text{--}206.3\ \mu\text{g kg}^{-1}$ ) for soil antibiotic pollution (Figure 3A).

However, the potential to meet the minimum regional demands for protecting soil biota within soil antibiotic pollution boundaries varies strongly across regions (Figures 3B and S8). High-income countries usually have lower regional boundaries, indicating a high burden of soil antibiotic pollution. These regions, which are usually located in middle-high latitude (include Europe and Eastern North America), are characterized by soils with the highest normalized abundance of antibiotic resistance genes.<sup>3</sup> Moreover, soil communities in the  $35^{\circ}\text{N}\text{--}40^{\circ}\text{N}$  region are more sensitive to environmental change.<sup>48</sup> Therefore, these low regional boundaries are mostly expected to occur in the global north, with high boundaries in the global south, across scenarios.

Next, we focus on priority areas where soil antibiotic susceptibility poses strong impacts on soil biota. Priority areas are identified with COSA exceeding the boundary values and a significant relationship ( $|t| > 1.96$ ) between COSA and the soil biota health indicator B-DAR (see Method). Extent of priority areas varies among future pathways (Figures 4 and S9). Globally, the net differences in priority areas between 2015 and 2070 range

from  $-36.1\%$  net losses under SSP1-RCP2.6 to  $2.2\%$  net gains under SSP5-RCP8.5. Large areas of losses and gains occur in high-income countries, with a net loss ( $-12.1\%$ ) under SSP1-RCP2.6 and a net gain ( $1.3\%$ ) under SSP5-RCP8.5. Eastern Europe and West Africa in particular will experience net gains under both SSP2-RCP4.5 and SSP5-RCP8.5 (Figure S10). Notably, there are regions that are priority areas both in present-day and in the future, particularly in high-income countries (ranging from  $26.7\%$  to  $32.3\%$  across three future scenarios). These areas are smallest in the sustainability scenario (SSP1-RCP2.6). In fact, the sustainability scenario shows fewer exceedances of the COSA boundary, with stronger net losses of priority areas, indicating low threats of damages on soil biota. SSP5-RCP8.5 will result in the largest net gains in priority areas, especially in South Asia. With the degradation of sanctuaries in SSP5-RCP8.5,<sup>26</sup> soil biodiversity might be more sensitive to the pressure of soil antibiotic pollution, which is expressed in net gains in priority areas. Together, these results indicate that there will be substantial shifts ( $-36.1\%$  net losses to  $2.2\%$  net gains) in the priority areas caused by soil antibiotic susceptibility because of future development options. Our findings also suggest that SSP1-RCP2.6 contribute to the reconciliation of soil biota health and compliance with the boundaries of soil antibiotic pollution; however, SSP5-RCP8.5 are accompanied by transgressions of safe boundaries.

In summary, our study underscores the pressing need to reduce soil antibiotic susceptibility for planetary health. By predicting global soil antibiotic concentrations under multiple future scenarios and defining planetary boundaries for soil antibiotic pollution, we provide novel insights into its spatial distribution and global impacts. We have not only identified critical global hotspots where soil antibiotic pollution threatens three dimensions of soil biota health (soil alpha diversity, community dissimilarity, and antibiotic resistance), but also revealed the co-existence of these three dimensions over  $20\%$  of global land areas. These findings establish critical thresholds for soil

antibiotic pollution, serving as a foundation for protecting soil biota health and understanding the dynamics of antibiotic contamination in a changing world.

### Limitations of the study

However, uncertainties remain, such as limited data from low-income regions, which may underestimate pollution levels, and unaccounted factors like advancements in pollutant-removal technologies or changes in global policies, potentially affecting our projections. Acknowledging these uncertainties, our work marks an initial step toward comprehending the global significance of threats posed by soil antibiotic pollution. It also suggests that the current priority areas where soil biota are strongly threatened by soil antibiotic susceptibility are sensitive to global change in the future. To address this, we recommend the mobilization of soil susceptibility mitigation strategies, facilitating governments and decision-makers in shaping global and regional conservation goals for soil biota in the future.

### RESOURCE AVAILABILITY

#### Lead contact

Further information and requests for resources should be directed to and will be fulfilled by the lead contact, Liding Chen ([liding@ynu.edu.cn](mailto:liding@ynu.edu.cn)).

#### Materials availability

This study did not generate any new physical materials.

#### Data and code availability

- All data needed to evaluate the conclusions in the paper are present in the paper and/or the Supplementary Materials. The raw data of antibiotic records are available in figshare (<https://doi.org/10.6084/m9.figshare.22793033.v2>).
- The codes for statistical analyses and visualization can be available from the corresponding authors upon reasonable request.
- Any additional information required to reanalyze the data reported in this paper is available from the [lead contact](#) upon request.

### ACKNOWLEDGMENTS

We acknowledge funding from the National Natural Science Foundation of China (grant 42201121, 42230718), Yunnan Provincial Science and Technology Project at Southwest United Graduate School (grant 202302AO370012), and Yunnan University (grant CZ22623101, CZ22621211).

### AUTHOR CONTRIBUTIONS

F.Z., L.Y., and L.C. designed the research; F.Z., L.Y., Yong Huang, Q.F., L.S., and M.L. performed research and collected data; F.Z. analyzed data; and F.Z., L.Y., Yuanyuan Huang, H.Y., and L.C. wrote and reviewed the paper.

### DECLARATION OF INTERESTS

The authors declare no competing interest.

### STAR★METHODS

Detailed methods are provided in the online version of this paper and include the following:

- [KEY RESOURCES TABLE](#)
- [METHOD DETAILS](#)
  - Database assembly and preprocessing
  - Global covariates and geospatial modeling

- Future projections
- Defining safe boundaries

### ● QUANTIFICATION AND STATISTICAL ANALYSIS

### SUPPLEMENTAL INFORMATION

Supplemental information can be found online at <https://doi.org/10.1016/j.isci.2025.112066>.

Received: November 4, 2024

Revised: December 18, 2024

Accepted: February 17, 2025

Published: February 20, 2025

### REFERENCES

1. Van Boeckel, T.P., Glennon, E.E., Chen, D., Gilbert, M., Robinson, T.P., Grenfell, B.T., Levin, S.A., Bonhoeffer, S., and Laxminarayan, R. (2017). Reducing antimicrobial use in food animals. *Science* 357, 1350–1352. <https://doi.org/10.1126/science.aao1495>.
2. Wilkinson, J.L., Boxall, A.B.A., Kolpin, D.W., Leung, K.M.Y., Lai, R.W.S., Galbán-Malagón, C., Adell, A.D., Mondon, J., Metian, M., Marchant, R.A., et al. (2022). Pharmaceutical pollution of the world's rivers. *Proc. Natl. Acad. Sci. USA* 119, e2113947119. <https://doi.org/10.1073/pnas.2113947119>.
3. Zheng, D., Yin, G., Liu, M., Hou, L., Yang, Y., Van Boeckel, T.P., Zheng, Y., and Li, Y. (2022). Global biogeography and projection of soil antibiotic resistance genes. *Sci. Adv.* 8, eabq8015. <https://doi.org/10.1126/sciadv.abq8015>.
4. Wepking, C., Badgley, B., Barrett, J.E., Knowlton, K.F., Lucas, J.M., Minick, K.J., Ray, P.P., Shawver, S.E., and Strickland, M.S. (2019). Prolonged exposure to manure from livestock-administered antibiotics decreases ecosystem carbon-use efficiency and alters nitrogen cycling. *Ecol. Lett.* 22, 2067–2076. <https://doi.org/10.1111/ele.13390>.
5. Larsson, D.G.J., and Flach, C.-F. (2022). Antibiotic resistance in the environment. *Nat. Rev. Microbiol.* 20, 257–269. <https://doi.org/10.1038/s41579-021-00649-x>.
6. Zhao, F., Yang, L., Yen, H., Feng, Q., Li, M., and Chen, L. (2023). Reducing risks of antibiotics to crop production requires land system intensification within thresholds. *Nat. Commun.* 14, 6094. <https://doi.org/10.1038/s41467-023-41258-x>.
7. Richmond, E.K., Rosi, E.J., Walters, D.M., Fick, J., Hamilton, S.K., Brodin, T., Sundelin, A., and Grace, M.R. (2018). A diverse suite of pharmaceuticals contaminates stream and riparian food webs. *Nat. Commun.* 9, 4491. <https://doi.org/10.1038/s41467-018-06822-w>.
8. Klein, E.Y., Van Boeckel, T.P., Martinez, E.M., Pant, S., Gandra, S., Levin, S.A., Goossens, H., and Laxminarayan, R. (2018). Global increase and geographic convergence in antibiotic consumption between 2000 and 2015. *Proc. Natl. Acad. Sci. USA* 115, 3463–3470. <https://doi.org/10.1073/pnas.1717295115>.
9. Van Boeckel, T.P., Brower, C., Gilbert, M., Grenfell, B.T., Levin, S.A., Robinson, T.P., Teillant, A., and Laxminarayan, R. (2015). Global trends in antimicrobial use in food animals. *Proc. Natl. Acad. Sci. USA* 112, 5649–5654. <https://doi.org/10.1073/pnas.1503141112>.
10. Richardson, K., Steffen, W., Lucht, W., Bendtsen, J., Cornell, S.E., Donges, J.F., Drüke, M., Fetzer, I., Bala, G., von Bloh, W., et al. (2023). Earth beyond six of nine planetary boundaries. *Sci. Adv.* 9, eadh2458. <https://doi.org/10.1126/sciadv.adh2458>.
11. Jørgensen, P.S., Aktipis, A., Brown, Z., Carrière, Y., Downes, S., Dunn, R.R., Epstein, G., Frisvold, G.B., Hawthorne, D., Gröhn, Y.T., et al. (2018). Antibiotic and pesticide susceptibility and the Anthropocene operating space. *Nat. Sustain.* 1, 632–641. <https://doi.org/10.1038/s41893-018-0164-3>.

12. Diamond, M.L., de Wit, C.A., Molander, S., Scheringer, M., Backhaus, T., Lohmann, R., Arvidsson, R., Bergman, Å., Hauschild, M., Holoubek, I., et al. (2015). Exploring the planetary boundary for chemical pollution. *Environ. Int.* 78, 8–15. <https://doi.org/10.1016/j.envint.2015.02.001>.
13. Toth, J.D., Feng, Y., and Dou, Z. (2011). Veterinary antibiotics at environmentally relevant concentrations inhibit soil iron reduction and nitrification. *Soil Biol. Biochem.* 43, 2470–2472. <https://doi.org/10.1016/j.soilbio.2011.09.004>.
14. Cairns, J., Jokela, R., Becks, L., Mustonen, V., and Hiltunen, T. (2020). Repeatable ecological dynamics govern the response of experimental communities to antibiotic pulse perturbation. *Nat. Ecol. Evol.* 4, 1385–1394. <https://doi.org/10.1038/s41559-020-1272-9>.
15. Santás-Miguel, V., Arias-Estévez, M., Díaz-Raviña, M., Fernández-Sanjurjo, M.J., Álvarez-Rodríguez, E., Núñez-Delgado, A., and Fernández-Calviño, D. (2020). Interactions between soil properties and tetracycline toxicity affecting to bacterial community growth in agricultural soil. *Appl. Soil Ecol.* 147, 103437. <https://doi.org/10.1016/j.apsoil.2019.103437>.
16. Nguyen, B.-A.T., Chen, Q.-L., He, J.-Z., and Hu, H.-W. (2020). Oxytetracycline and ciprofloxacin exposure altered the composition of protistan consumers in an agricultural soil. *Environ. Sci. Technol.* 54, 9556–9563. <https://doi.org/10.1021/acs.est.0c02531>.
17. Sharma, U., Rawat, D., Mukherjee, P., Farooqi, F., Mishra, V., and Sharma, R.S. (2023). Ecological life strategies of microbes in response to antibiotics as a driving factor in soils. *Sci. Total Environ.* 854, 158791. <https://doi.org/10.1016/j.scitotenv.2022.158791>.
18. Pino-Otin, M.R., Muniz, S., Val, J., and Navarro, E. (2017). Effects of 18 pharmaceuticals on the physiological diversity of edaphic microorganisms. *Sci. Total Environ.* 595, 441–450. <https://doi.org/10.1016/j.scitotenv.2017.04.002>.
19. Chen, Z., Zhang, W., Peng, A., Shen, Y., Jin, X., Stedtfeld, R.D., Boyd, S.A., Teppen, B.J., Tiedje, J.M., Gu, C., et al. (2023). Bacterial community assembly and antibiotic resistance genes in soils exposed to antibiotics at environmentally relevant concentrations. *Environ. Microbiol. Environ. Microbiol.* 25, 1439–1450. <https://doi.org/10.1111/1462-2920.16371>.
20. Peng, Z., Qian, X., Liu, Y., Li, X., Gao, H., An, Y., Qi, J., Jiang, L., Zhang, Y., Chen, S., et al. (2024). Land conversion to agriculture induces taxonomic homogenization of soil microbial communities globally. *Nat. Commun.* 15, 3624. <https://doi.org/10.1038/s41467-024-47348-8>.
21. Ma, J., Zhu, D., Sheng, G.D., O'Connor, P., and Zhu, Y.-G. (2019). Soil oxytetracycline exposure alters the microbial community and enhances the abundance of antibiotic resistance genes in the gut of *Enchytraeus crypticus*. *Sci. Total Environ.* 673, 357–366. <https://doi.org/10.1016/j.scitotenv.2019.04.103>.
22. Perry, E.K., Meirelles, L.A., and Newman, D.K. (2022). From the soil to the clinic: the impact of microbial secondary metabolites on antibiotic tolerance and resistance. *Nat. Rev. Microbiol.* 20, 129–142. <https://doi.org/10.1038/s41579-021-00620-w>.
23. Zhu, Y.-G., Zhao, Y., Zhu, D., Gillings, M., Penueles, J., Ok, Y.S., Capon, A., and Banwart, S. (2019). Soil biota, antimicrobial resistance and planetary health. *Environ. Int.* 131, 105059. <https://doi.org/10.1016/j.envint.2019.105059>.
24. Zhang, Q., Zhang, G., Liu, D., Zhang, X., Fang, R., Wang, L., Chen, Y., Lin, L., Wu, H., and Li, S. (2022). A dataset of distribution of antibiotic occurrence in solid environmental matrices in China. *Sci. Data* 9, 276. <https://doi.org/10.1038/s41597-022-01384-5>.
25. Spets, P., Ebert, K., and Dinnézt, P. (2023). Spatial analysis of antimicrobial resistance in the environment. A systematic review. *Geospatial Health* 18, 1168. <https://doi.org/10.4081/gh.2023.1168>.
26. Guerra, C.A., Berdugo, M., Eldridge, D.J., Eisenhauer, N., Singh, B.K., Cui, H., Abades, S., Alfaro, F.D., Bamigboye, A.R., Bastida, F., et al. (2022). Global hotspots for soil nature conservation. *Nature* 610, 693–698. <https://doi.org/10.1038/s41586-022-05292-x>.
27. Borrelli, P., Robinson, D.A., Panagos, P., Lugato, E., Yang, J.E., Alewell, C., Wuepper, D., Montanarella, L., and Ballabio, C. (2020). Land use and climate change impacts on global soil erosion by water (2015–2070). *Proc. Natl. Acad. Sci. USA* 117, 21994–22001. <https://doi.org/10.1073/pnas.2001403117>.
28. O'Neill, B.C., Tebaldi, C., van Vuuren, D.P., Eyring, V., Friedlingstein, P., Hurtt, G., Knutti, R., Kriegler, E., Lamarque, J.F., Lowe, J., et al. (2016). The Scenario Model Intercomparison Project (ScenarioMIP) for CMIP6. *Geosci. Model Dev. (GMD)* 9, 3461–3482. <https://doi.org/10.5194/gmd-9-3461-2016>.
29. Menz, J., Olsson, O., and Kümmerer, K. (2019). Antibiotic residues in live-stock manure: Does the EU risk assessment sufficiently protect against microbial toxicity and selection of resistant bacteria in the environment? *J. Hazard Mater.* 379, 120807. <https://doi.org/10.1016/j.jhazmat.2019.120807>.
30. Taylor, P., and Reeder, R. (2020). Antibiotic use on crops in low and middle-income countries based on recommendations made by agricultural advisors. *CABI Agric. Biosci.* 1, 1. <https://doi.org/10.1186/s43170-020-00001-y>.
31. Jones, K.E., Patel, N.G., Levy, M.A., Storeygard, A., Balk, D., Gittleman, J.L., and Daszak, P. (2008). Global trends in emerging infectious diseases. *Nature* 451, 990–993. <https://doi.org/10.1038/nature06536>.
32. Abat, C., Gautret, P., and Raoult, D. (2018). Benefits of antibiotics burden in low-income countries. *Proc. Natl. Acad. Sci. USA* 115, E8109–E8110. <https://doi.org/10.1073/pnas.1809354115>.
33. Hendriksen, R.S., Munk, P., Njage, P., van Bunnik, B., McNally, L., Lukjancenko, O., Röder, T., Nieuwenhuijse, D., Pedersen, S.K., Kjeldgaard, J., et al. (2019). Global monitoring of antimicrobial resistance based on metagenomics analyses of urban sewage. *Nat. Commun.* 10, 1124. <https://doi.org/10.1038/s41467-019-08853-3>.
34. Zhang, B., Tian, H., Lu, C., Dangal, S.R.S., Yang, J., and Pan, S. (2017). Global manure nitrogen production and application in cropland during 1860–2014: a 5 arcmin gridded global dataset for Earth system modeling. *Earth Syst. Sci. Data* 9, 667–678. <https://doi.org/10.5194/essd-9-667-2017>.
35. Wu, J., Wang, J., Li, Z., Guo, S., Li, K., Xu, P., Ok, Y.S., Jones, D.L., and Zou, J. (2023). Antibiotics and antibiotic resistance genes in agricultural soils: A systematic analysis. *Crit. Rev. Environ. Sci. Technol.* 53, 847–864. <https://doi.org/10.1080/10643389.2022.2094693>.
36. Oldenkamp, R., Huijbregts, M.A.J., Hollander, A., Versporten, A., Goossens, H., and Ragas, A.M.J. (2013). Spatially explicit prioritization of human antibiotics and antineoplastics in Europe. *Environ. Int.* 51, 13–26. <https://doi.org/10.1016/j.envint.2012.09.010>.
37. Tang, F.H.M., Lenzen, M., McBratney, A., and Maggi, F. (2021). Risk of pesticide pollution at the global scale. *Nat. Geosci.* 14, 206–210. <https://doi.org/10.1038/s41561-021-00712-5>.
38. Allel, K., Day, L., Hamilton, A., Lin, L., Furuya-Kanamori, L., Moore, C.E., Van Boeckel, T., Laxminarayan, R., and Yakob, L. (2023). Global antimicrobial-resistance drivers: an ecological country-level study at the human-animal interface. *Lancet Planet. Health* 7, e291–e303. [https://doi.org/10.1016/S2542-5196\(23\)00026-8](https://doi.org/10.1016/S2542-5196(23)00026-8).
39. Chua, P.L.C., Huber, V., Ng, C.F.S., Seposo, X.T., Madaniyazi, L., Hales, S., Woodward, A., and Hashizume, M. (2021). Global projections of temperature-attributable mortality due to enteric infections: a modelling study. *Lancet Planet. Health* 5, e436–e445. [https://doi.org/10.1016/S2542-5196\(21\)00152-2](https://doi.org/10.1016/S2542-5196(21)00152-2).
40. Trinanès, J., and Martínez-Urtaza, J. (2021). Future scenarios of risk of Vibrio infections in a warming planet: a global mapping study. *Lancet Planet. Health* 5, e426–e435. [https://doi.org/10.1016/S2542-5196\(21\)00169-8](https://doi.org/10.1016/S2542-5196(21)00169-8).
41. Georgiou, K., Jackson, R.B., Vindusková, O., Abramoff, R.Z., Ahlström, A., Feng, W., Harden, J.W., Pellegrini, A.F.A., Polley, H.W., Soong, J.L., et al. (2022). Global stocks and capacity of mineral-associated soil organic carbon. *Nat. Commun.* 13, 3797. <https://doi.org/10.1038/s41467-022-31540-9>.



42. Zhu, Y., Yang, Q., Lu, T., Qi, W., Zhang, H., Wang, M., Qi, Z., and Chen, W. (2020). Effect of phosphate on the adsorption of antibiotics onto iron oxide minerals: Comparison between tetracycline and ciprofloxacin. *Ecotoxicol. Environ. Saf.* 205, 111345. <https://doi.org/10.1016/j.ecoenv.2020.111345>.
43. Cerqueira, F., Christou, A., Fatta-Kassinos, D., Vila-Costa, M., Bayona, J.M., and Piña, B. (2020). Effects of prescription antibiotics on soil- and root-associated microbiomes and resistomes in an agricultural context. *J. Hazard Mater.* 400, 123208. <https://doi.org/10.1016/j.jhazmat.2020.123208>.
44. Ma, J., Sheng, G.D., and O'Connor, P. (2020). Microplastics combined with tetracycline in soils facilitate the formation of antibiotic resistance in the *Enchytraeus crypticus* microbiome. *Environ. Pollut.* 264, 114689. <https://doi.org/10.1016/j.envpol.2020.114689>.
45. Ord, J.K., and Getis, A. (1995). Local Spatial Autocorrelation Statistics: Distributional Issues and an Application. *Geogr. Anal.* 27, 286–306. <https://doi.org/10.1111/j.1538-4632.1995.tb00912.x>.
46. Guerra, C.A., Delgado-Baquerizo, M., Duarte, E., Marigliano, O., Görgen, C., Maestre, F.T., and Eisenhauer, N. (2021). Global projections of the soil microbiome in the Anthropocene. *Global Ecol. Biogeogr.* 30, 987–999. <https://doi.org/10.1111/geb.13273>.
47. Mace, G.M., Reyers, B., Alkemade, R., Biggs, R., Chapin, F.S., Cornell, S.E., Diaz, S., Jennings, S., Leadley, P., Mumby, P.J., et al. (2014). Approaches to defining a planetary boundary for biodiversity. *Glob. Environ. Change* 28, 289–297. <https://doi.org/10.1016/j.gloenvcha.2014.07.009>.
48. Kuang, J., Deng, D., Han, S., Bates, C.T., Ning, D., Shu, W., and Zhou, J. (2022). Resistance potential of soil bacterial communities along a biodiversity gradient in forest ecosystems. *mLife* 7, 399–411. <https://doi.org/10.1002/mlf2.12042>.
49. Zhang, Y., Cheng, D., Xie, J., Zhang, Y., Wan, Y., Zhang, Y., and Shi, X. (2022). Impacts of farmland application of antibiotic-contaminated manures on the occurrence of antibiotic residues and antibiotic resistance genes in soil: A meta-analysis study. *Chemosphere* 300, 134529. <https://doi.org/10.1016/j.chemosphere.2022.134529>.
50. Tadić, Đ., Bleda Hernandez, M.J., Cerqueira, F., Matamoros, V., Piña, B., and Bayona, J.M. (2021). Occurrence and human health risk assessment of antibiotics and their metabolites in vegetables grown in field-scale agricultural systems. *J. Hazard Mater.* 401, 123424. <https://doi.org/10.1016/j.jhazmat.2020.123424>.
51. van den Hoogen, J., Geisen, S., Routh, D., Ferris, H., Traunsperger, W., Wardle, D.A., de Goede, R.G.M., Adams, B.J., Ahmad, W., Andriuzzi, W.S., et al. (2019). Soil nematode abundance and functional group composition at a global scale. *Nature* 572, 194–198. <https://doi.org/10.1038/s41586-019-1418-6>.
52. Cao, Y., Geddes, T.A., Yang, J.Y.H., and Yang, P. (2020). Ensemble deep learning in bioinformatics. *Nat. Mach. Intell.* 2, 500–508. <https://doi.org/10.1038/s42256-020-0217-y>.
53. Kuhn, M. (2008). Building Predictive Models in R Using the caret Package. *J. Stat. Software* 28, 1–26. <https://doi.org/10.18637/jss.v028.i05>.
54. Steffen, W., Richardson, K., Rockström, J., Cornell, S.E., Fetzer, I., Bennett, E.M., Biggs, R., Carpenter, S.R., de Vries, W., de Wit, C.A., et al. (2015). Planetary boundaries: Guiding human development on a changing planet. *Science* 347, 1259855. <https://doi.org/10.1126/science.1259855>.
55. Persson, L., Carney Almroth, B.M., Collins, C.D., Cornell, S., de Wit, C.A., Diamond, M.L., Fantke, P., Hasselöv, M., MacLeod, M., Ryberg, M.W., et al. (2022). Outside the safe operating space of the planetary boundary for novel entities. *Environ. Sci. Technol.* 56, 1510–1521. <https://doi.org/10.1021/acs.est.1c04158>.
56. Zhao, F., Yang, L., Yen, H., Yu, X., Fang, L., Li, M., and Chen, L. (2022). Can agricultural land use alter the responses of soil biota to antibiotic contamination? *J. Hazard Mater.* 437, 129350. <https://doi.org/10.1016/j.jhazmat.2022.129350>.
57. Sidhu, H., O'Connor, G., Ogram, A., and Kumar, K. (2019). Bioavailability of biosolids-borne ciprofloxacin and azithromycin to terrestrial organisms: Microbial toxicity and earthworm responses. *Sci. Total Environ.* 650, 18–26. <https://doi.org/10.1016/j.scitotenv.2018.09.004>.
58. Delgado-Baquerizo, M., Hu, H.-W., Maestre, F.T., Guerra, C.A., Eisenhauer, N., Eldridge, D.J., Zhu, Y.-G., Chen, Q.-L., Trivedi, P., Du, S., et al. (2022). The global distribution and environmental drivers of the soil antibiotic resistome. *Microbiome* 10, 219. <https://doi.org/10.1186/s40168-022-01405-w>.
59. Brunsdon, C., Fotheringham, A.S., and Charlton, M.E. (1996). Geographically Weighted Regression: A Method for Exploring Spatial Nonstationarity. *Geogr. Anal.* 28, 281–298. <https://doi.org/10.1111/j.1538-4632.1996.tb00936.x>.
60. Páez, A., Farber, S., and Wheeler, D. (2011). A Simulation-Based Study of Geographically Weighted Regression as a Method for Investigating Spatially Varying Relationships. *Environ. Plann.* 43, 2992–3010. <https://doi.org/10.1068/a44111>.
61. Bates, D.M., and Watts, D.G. (1988). *Nonlinear Regression Analysis and its Applications* (Wiley).
62. Muggeo, V.M.R. (2003). Estimating regression models with unknown break-points. *Stat. Med.* 22, 3055–3071. <https://doi.org/10.1002/sim.1545>.
63. Puth, M.-T., Neuhäuser, M., and Ruxton, G.D. (2015). On the variety of methods for calculating confidence intervals by bootstrapping. *J. Anim. Ecol.* 84, 892–897. <https://doi.org/10.1111/1365-2656.12382>.



## STAR★METHODS

## KEY RESOURCES TABLE

REAGENT or RESOURCE	SOURCE	IDENTIFIER
Deposited data		
Raw data of antibiotic records	figshare	<a href="https://doi.org/10.6084/m9.figshare.22793033.v2">https://doi.org/10.6084/m9.figshare.22793033.v2</a>
Software and algorithms		
ArcGIS 10.6	ESRI	<a href="https://www.arcgis.com/index.html">https://www.arcgis.com/index.html</a>
R 4.2.2	R Development Core Team	<a href="https://www.r-project.org/">https://www.r-project.org/</a>

## METHOD DETAILS

## Database assembly and preprocessing

We assembled previously published databases with records of the occurrence of antibiotics,<sup>6,24,35,49</sup> and collected data on antibiotic concentrations in soils across the globe. Studies and datasets included in these databases were selected according to several criteria: (1) study was not duplicate, and duplicate records were checked and eliminated; (2) only soil-associated samples (on average 10 cm of soil depth) were retained, and solid manure or waste samples were excluded; (3) soil samples that were not cultured or experimentally treated were included. However, soils treated by manure fertilization and wastewater irrigation, which corresponded to local land management practices, were not excluded; (4) geospatial information on sampling sites (latitude and longitude) was either directly provided in the original data or extracted through georeferencing using known maps, identifiable landmarks, and satellite imagery where necessary; (5) antibiotic concentrations for each sampling sites were provided (or average values for replicates), and concentrations that were “not detected” or “below detection limit” were assigned zero values; (6) rather than all antibiotics, we mainly focused on environmental concentrations of tetracyclines, quinolones, and sulfonamides antibiotics (target antibiotics are listed in Table S1) in soils, as they were widely and frequently detected worldwide.<sup>35</sup> Applying these criteria yielded a final dataset comprising 659 locations, from which we collected 1,351 soil samples (Figure S11), providing a comprehensive representation of environmental and anthropogenic variations in global agricultural regions.

## Global covariates and geospatial modeling

To understand controls of soil antibiotic pollution, a prepared stack of 24 global covariates relevant to society and the environment that could potentially affect antibiotic concentration (e.g., antibiotic use<sup>2</sup> and land cover<sup>50</sup>) were sampled at each location within our dataset.<sup>51</sup> These layers included anthropogenic, climatic, soil, and topographic variables and two other covariates (Table S2). All covariate layers were resampled at a 0.25° × 0.25° resolution. Before modeling, we removed outliers (2.5 times the standard deviation) from our compiled log10-transformed dataset to avoid potential biases, which resulted in the elimination of 15 records. Then, multiple child models based on machine-learning algorithms were trained to examine the associations between soil antibiotic concentrations and social/environmental covariates, as a single model usually has lower generalizability than a combination of multiple models.<sup>52</sup> We used four classes of child models: random forest, neural network, supporting vector machine, and partial least-squares regression models. Child models were fitted using a 10-fold cross-validation to prevent overfitting and to ensure extrapolation capacities outside the training datasets. A 10% subset of the data was extracted for validation, and the remaining 90% subset was used for training. The train and validation processes of all child models were bootstrapped 10 times to test their performance. The coefficient of determination ( $R^2$ ) values ranged from 0.71 to 0.88 (Figure S12), and random forest was suggested with better performance. Afterward, we averaged the outputs from individual child models, which enabled the multifaceted abstraction of data and better model outcomes.<sup>52</sup> We trained separate models for predicting tetracyclines, quinolones, and sulfonamides concentrations respectively. On average, agricultural activities and urbanization accounted for more relative influences on tetracyclines and quinolones concentrations, while soil conditions influenced sulfonamides concentration substantially (Figures S13 and S14).

Beyond data availability, the choice of 2015 as the baseline year is also informed by the need to establish a reference point that aligns with the onset of significant anthropogenic activities particularly the Sustainable Development Goals released in 2015. After, we adopted efforts to ensure our planet on the path of sustainable development. Using the global covariates and trained child models, we extrapolated the tetracyclines, quinolones, and sulfonamides concentrations in each pixel at a global scale, while excluding pixels completely covered by primary forests, waterbodies, deserts, or impervious surfaces to avoid our model projecting far outside its training dataset. The extent of agricultural land is from the ref.<sup>37</sup>, which illustrates the maximum likelihood in areas with active ingredient use (resolution: 5 arcmin). The cumulative antibiotic concentration was calculated by summing concentrations of tetracyclines, quinolones, and sulfonamides according to the concentration addition principle.<sup>36</sup> The each-pixel mean value and standard deviation were calculated based on the results of four child models. Using these values, the bootstrap prediction

uncertainties of our models were characterized by the coefficient of variation (standard deviation divided by mean value). Based on the bootstrap procedure, 10 generated images were used to estimate per-pixel uncertainties of selected antibiotics for four classes of child models respectively (Figure S15). To assess the model differences, we further calculated the per-pixel mean values of each child model, and then the coefficient of variation values are generated among the four child models to show the prediction robustness across different models (Figure S1). We created final global maps of soil antibiotic pollution by model averaging. The geospatial modeling procedure was performed in the *Caret*<sup>53</sup> package in R.

### Future projections

All temporal changes (2015–2070) were calculated using 2015 as a baseline and 2070 as a endpoint. The selection of 2070 as the endpoint to assess temporal changes in soil antibiotic pollution is grounded in its alignment with policy frameworks and modeling conventions. By extending projections to this medium-term time frame, we can adequately capture evolving trends critical for informing future policy interventions and sustainable management practices. This choice resonates with broader studies that utilize the 2015–2070 period to assess temporal changes on our planet,<sup>26,27</sup> facilitating informed decision-making and promoting sustainable practices for environmental stewardship.

We selected three representative combinations of Shared Socioeconomic Pathway (SSP) and Representative Concentration Pathway (RCP) scenarios (SSP1-RCP2.6, SSP2-RCP4.5, and SSP5-RCP8.5) to understand the changes in soil antibiotic pollution until 2070. The SSP-RCP framework is widely regarded as a gold standard for integrating socioeconomic and climate projections, allowing us to assess how different socio-economic trajectories influence soil antibiotic pollution and mitigation efforts. We prioritized SSPs that address challenges related to mitigation, enabling us to evaluate strategies within the broader context of sustainable development and their potential to reduce soil antibiotic pollution. Below, we summarize the main characteristics of the selected scenarios that are potentially related to antibiotic pollutions.<sup>28</sup>

- (1) SSP1-RCP2.6 (Global Sustainable Development): This scenario represents a green development paradigm. Population growth is moderate to slow by mid-century, and climate policies are implemented to limit the average global temperature increase to a maximum of 2°C. Agricultural land is projected to significantly decrease, and forest cover is expected to increase, reflecting a shift toward sustainable land use practices.
- (2) SSP2-RCP4.5 (Intermediate Pathway): This scenario reflects a middle-of-the-road development pathway, with moderate land-use changes and temperature increases. It combines intermediate societal vulnerability with moderate challenges for climate change mitigation, offering a balanced perspective on future trajectories.
- (3) SSP5-RCP8.5: This scenario represents a resource-intensive development model characterized by rapid economic growth, high fossil fuel use, and significant global warming. Increased food demand and intensified livestock production drive the expansion of agricultural land into pasture and forested areas, significantly impacting soil health.

The global covariate layers generally have large time ranges (from 2015 to 2070) for the three future scenarios, except antibiotic use and livestock density data (Table S2). We performed extra analyses to obtain predicted data for the future. As antibiotic use and livestock density are both functions of population demand, we assumed that they would have the same annual growth rates as the rate of population increase from 2015 to 2070 for each country.<sup>8,9</sup> Countries were selected and classified using administrative boundaries to ensure consistent and comparable geographical analysis. The projected antibiotic use and livestock densities for 2070 were estimated by multiplying their values per pixel in 2015 by the growth rate, that can minimize the influences of other environmental factors which also affect population size. Finally, we repeated the geospatial prediction to map global antibiotic concentrations in each pixel under different future scenarios (Figure S16).

### Defining safe boundaries

The safe boundaries define limits that should not be transgressed to maintain sustainability. Control and response variables are required to quantify the boundary values.<sup>54</sup> Given the interactions between antibiotic pollution and biodiversity, here, we define the control variable as the concentrations of antibiotics (COSA), and the response variable as the decrease in biota health,<sup>47,55</sup> of which we selected microbes (mainly including bacteria and fungi), invertebrates, and antibiotic resistance genes (ARGs) as targets because of their higher sensitivity to antibiotic pressures than the others.<sup>56,57</sup> The global layers (about 0–10 cm depth) of alpha diversity and community dissimilarity (community heterogeneity, as measured by Jaccard distance) of bacteria, fungi, and invertebrates have been well projected at 2015 and 2070 in a recent global assessment, and were publicly available.<sup>26</sup> These datasets were obtained from global field surveys following standardized field protocols, which contained 615 soil samples covering 151 locations from all continents and 23 countries (Figure S11). Although the layer of ARGs richness was only available at present-day, we used the global dataset and model established by Delgado-Baquerizo et al.<sup>58</sup> to project the 2070 layer (Figure S11). The ARGs field survey were collected from 1012 sites from 35 countries across all continents. We selected these two datasets for three main reasons: (1) the data in each dataset were measured from the same samples using the same protocols; (2) these datasets covered a large portion of the large-scale environmental variability of the planet providing a large representation of climatic and vegetation conditions on the planet.

Before the quantification of safe boundaries, we standardized all gridded layers to a range of 0–1 using the equation:  $y = (x - x_{min}) / (x_{max} - x_{min})$ . The biodiversity of soil biota was estimated from the sum of the standardized alpha diversity scores of bacteria, fungi, and invertebrates, and the dissimilarity was the sum of their standardized Jaccard distance scores. Due to the negative relationships between ARGs richness and biota health, the standardized scores of ARGs were reversed using the equation:  $y = (x_{min} - x) / (x_{max} - x_{min})$ . After standardization, soil biota health was calculated as the cumulative score of Biodiversity, Dissimilarity, and reversed Antibiotic Resistance gene richness (B-DAR) at each grid, using equal weighting to avoid bias and ensure all dimensions contribute equally to the assessment. We use B-DAR to represent this integrated indicator of soil biota health.

To quantify the boundaries, we carried out five analyses at different spatial resolutions ( $1^\circ$ ,  $1.5^\circ$ ,  $2^\circ$ ,  $2.5^\circ$ , and  $3^\circ$ ) to assess the sensitivity to spatial resolutions. At each resolution, we estimated the impact strength between antibiotic pollution and biota health at each pixel using geographically weighted regression (*spgwr* package), which was preferred for its ability to capture spatial non-stationarity and reveal localized variations in relationships across geographical space.<sup>59,60</sup> A fixed Gaussian kernel was employed to identify the best bandwidth based on the lowest corrected Akaike information criterion. The regression slope in each pixel was recorded as the impact strength, which indicated an increase (positive slope) or decrease (negative slope) in soil biota health with increasing antibiotic pollution. The global cluster of regression slope was calculated using the Getis-Ord  $G_i^*$  method (Z score),<sup>45</sup> for which a high Z score meant a high probability of a cluster of positive slope values, and a low Z score (usually negative) indicated negative slope values that are spatially clustered. Specifically, the fine-resolution ( $1^\circ \times 1^\circ$ ) models generated higher local  $R^2$  values than coarse-resolution models, indicating better model performance (Figure S17).

We ranked all  $1^\circ \times 1^\circ$  pixels from lowest to highest according to COSA. Then, we calculated the average COSA and cumulative decrease in biota health (sum of impact strengths) from the top 0%–100% pixels. The cumulative decrease in biota health was plotted against the average COSA, and their relationship was described by the following curve:

$$y = a + \frac{(b - a)}{1 + (x/c)^d}$$

where  $x$  and  $y$  are the control variable and response variable, respectively, and  $a$ ,  $b$ ,  $c$ ,  $d$  are fitting parameters. The best parameter combination was estimated using a nonlinear least squares method (via the *stats* package in R).<sup>61</sup> Nonlinear relationships can be considered as piecewise straight lines. We defined the global boundary values as the breakpoint for  $x$  on the curve, which was identified as the point at which the linear relationship significantly changed based on the slope parameters (using the *segmented* package).<sup>62</sup> In addition, we further identified regional boundaries by repeating the curve estimation and breakpoint identification procedures using data from within each region or country.

## QUANTIFICATION AND STATISTICAL ANALYSIS

The global mean of soil antibiotic concentration was estimated by averaging the predicted values of all pixels from 10 child models. The 95% confidence intervals were derived by bootstrap technique due to the non-normally distributed data. The 1000 times bootstraps were performed using non-parametric method, which makes no assumptions of data distribution. A 95% bootstrap confidence interval formed from the 2.5th and 97.5th percentiles of a set of 1000 bootstrapped estimates.<sup>63</sup> We also calculated the mean values and 95% confidence interval based on the countries' income level (please see Figure 1 and its legend). The statistical analyses were performed in R 4.2.2.